Research Article | Vol. 27, No. 23 / 11 November 2019 / Optics Express 33427
Optics EXPRESS

Observation of 2D semiconductor P-type dark-exciton lifetime using two-photon ultrafast spectroscopy

DMITRY PANNA,[1] KRISHNA BALASUBRAMANIAN,[1,*] JAYAKRISHNA KHATEI,[1,3] LEONID RYBAK,[1] YEVGENY SLOBODKIN,[2] HADAR STEINBERG,[2] AND ALEX HAYAT[1]

[1]Department of Electrical Engineering, Technion, Haifa 32000, Israel
[2]Racah Institute of Physics, The Hebrew University of Jerusalem, Jerusalem 91904, Israel
[3]Department of Physics, CET, Bhubaneswar, India
[*]krishnab@campus.technion.ac.il

Abstract: We report direct measurements of intrinsic lifetimes of P-type dark-excitons in MoS_2 monolayers. Using sub-gap excitation, we demonstrate two-photon excited direct population of P-type dark excitons, observe their scattering to bright states and decay with femtosecond resolution. In contrast to one-photon excitation schemes, non-monotonic density variation in bright exciton population observed under two-photon excitation shows the indirect nature of its population and competing decay pathways. Detailed modeling of different recombination pathways of bright and dark excitons allows experimental measurement of 2P dark → 1S bright exciton scattering rates. These insights into the dark states in a MoS_2 monolayer pave the way for novel devices such as quantum memories and computing.

1. Introduction

Transition metal dichalcogenide (TMD) monolayers host strongly bound excitons which are stable at room temperature and exhibit a wide range of interesting properties [1,2]. Monolayers of TMDs are semiconductors with a direct bandgap in visible and near-infrared ranges making them attractive for optoelectronic applications [3]. Optical properties of various monolayers have been well studied and shown to exhibit exciting phenomena such as circular dichroism [4] and the valley-Hall effect [5]. In order to understand fundamental mechanisms of carrier dynamics, several time-resolved studies have been performed revealing multi-exponential decays indicating various competing relaxation pathways [6,7]. These studies deduced important characteristic times of various recombination mechanisms at room and cryogenic temperatures. The experimentally measured photoluminescence decay times [8] in these TMDs at room temperature [9] were significantly longer than the theoretical predictions (~270 ps [10]). In contrast, at low temperatures, the observed lifetime matched closely to calculated values [11]. Recently, the mismatch between the calculated and observed values at room temperature was attributed to dark-exciton states [12]. These dark states participate in the bright-exciton dynamics at room temperature leading to longer than calculated effective lifetimes. In monolayer TMDs, three types of dark excitons exist: the spin-mismatched excitons, non-zero orbital angular momentum excitons, and excitons away from the light cone [13]. Spin forbidden dark-exciton states in monolayer TMDs are predicted to lie close to the bright states (within the thermal energy range at room temperature) with the lowest excited state being dark or bright in WSe_2 or MoS_2 respectively [14]. Using an external magnetic field, the spin-forbidden dark-bright exciton splitting for TMDs was found experimentally to agree with the calculated value [15,16]. However, the lowest non-zero orbital angular momentum dark exciton state (P-type) in MoS_2 is predicted to be 0.17 eV above the 1S state for A exciton and 0.21 eV for the B exciton [17]. While the direct

#374404 https://doi.org/10.1364/OE.27.033427
Journal © 2019 Received 6 Aug 2019; revised 21 Sep 2019; accepted 21 Sep 2019; published 31 Oct 2019

Optics EXPRESS

population of such dark states was demonstrated [18], their dynamics and subsequent decay studies, which have not been reported yet, can aid in design and development of applications such as quantum memories based on P-type dark excitonic states.

Here, we directly measure the P-type dark-exciton lifetime, by performing two-photon pump and one-photon probe experiments on MoS_2 monolayers to excite non-zero orbital angular momentum dark excitons (P-type) and probe the (1S) bright-exciton population dynamics on femtosecond timescale. Two-photon excitation has been shown experimentally to selectively couple to the P-type dark-exciton states in TMDs [18]. Using a pump pulse, significantly red-detuned relative to the dark-exciton energy, we generate P-type dark-exciton population through the two-photon absorption process. A white-light supercontinuum probe pulse measures bright exciton dynamics at various energies and pump-probe delay times. Since the P-type dark exciton is forbidden to recombine via one-photon processes, the non-radiative recombination rate and, most importantly, the recombination via scattering to lower energy bright state (1S) determine the lifetime of this type of dark exciton. Furthermore, we performed one-photon pump-probe experiments to extract the relevant bright excitonic lifetimes. We carried out a detailed rate analysis of the bright and the dark exciton relaxation and scattering mechanisms to extract the individual decay rates. The extracted bright exciton radiative and Auger recombination rates match the reported values, validating our model. Moreover, we show and contrast dark and bright exciton population dynamics with fs resolution under the aforementioned excitation schemes. Using such a direct measurement we find the 2P-dark $\rightarrow$ bright exciton scattering time in MoS_2 to be 72.5 ps. In addition to influencing photoluminescence decay time, the interplay between the dark and bright-exciton states also leads to radically different optical properties such as photoluminescence (PL) polarization among the TMD material family members [19]. Detailed understanding of the excitonic lifetimes and dynamics can enable development of practical excitonic devices [20] and novel applications such as quantum memories [21].

2. Methods

For our experiments, the MoS_2 monolayer samples were mechanically exfoliated onto a SiO_2 substrate from undoped bulk MoS_2 crystals. In our pump-probe setup, a 1 kHz Ti:Sapphire regenerative amplifier delivers 35 fs pulses at 1.55 eV (800 nm). The laser output was split into two linearly polarized beams: the first one is fed to an optical parametric amplifier (OPA), which serves as the wavelength-tunable pump and the second one generates broadband supercontinuum in a single-crystal sapphire plate for the probe. The white-light impinges on the sample at almost normal incidence and is reflected into a spectrometer, which allows us to deduce reflectivity changes induced by the pump as depicted in Fig. 1. Subsequently, a motorized translation stage varies the pump-probe time delay and a pair of quarter-wave plates controls both pulses. The probe signal spot size was set to 30 µm and the pump signal spot size overlapping the probe was about 1 mm. The integration time of the detector was 10 ms and the time resolution observed was about 100 fs. Several flakes were inspected and a flake, identified using Raman and photoluminescence, was used to conduct all the measurements reported.

Reflectivity at normal incidence from the interface between two media with complex refractive indices n_1 and n_2 is given by [22]

$$R = \left| \frac{n_2 - n_1}{n_2 + n_1} \right|^2 \tag{1}$$

The complex refractive index is defined as $n = \sqrt{\epsilon}$, where the ϵ is the complex dielectric function at an optical frequency ω, and $\epsilon(\omega) = \epsilon_r(\omega) + i\epsilon_i(\omega)$. The real ($\epsilon_r(\omega)$) and the imaginary parts ($\epsilon_i(\omega)$) of the dielectric constant are related by the Kramers-Kronig relation. In the pump-probe experiment the pump pulse generates the excitonic population, changing the absorption of the following probe pulse. This change is time-dependent as the pump excited carriers decay, and is monitored through the reflectivity changes according to Eq. (1).

Optics EXPRESS

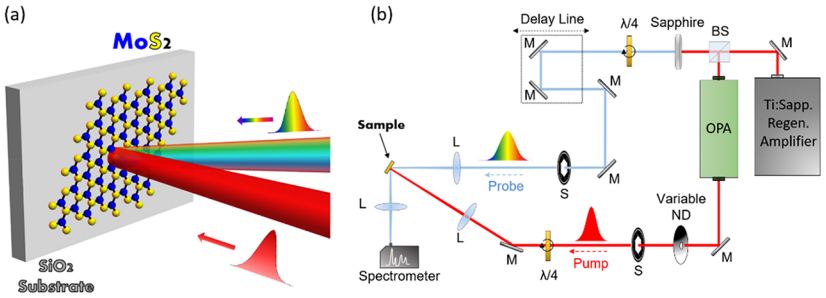

Fig. 1. (a). Illustration of a MoS_2 sample transferred onto a SiO_2 substrate and the pump (red) and the probe (rainbow colors) beams impinging on the sample. **(b).** Schematic drawing of the experimental setup: OPA - optical parametric amplifier, BS - beam splitter; M - mirror; S - shutter, L - plano-convex lens, ND - neutral density filter, $\lambda/4$ – quarter wave plate.

3. Results and Discussion

We first performed a one-photon pump-probe experiment, generating carriers in the conduction band and observing subsequent ultrafast exciton dynamics. The monolayer of MoS_2 was excited by 35 fs pump pulses with photon energy of 2.55 eV and fluence of 337μJ/cm^2. This excitation wavelength was chosen to populate both the A and B exciton series simultaneously. Such as scheme was chosen over resonant excitation to extract population dynamics of both A and B as these one-photon experiments were conducted to serve as a benchmark for the subsequently two-photon measurements. In contrast to the pump, the probe pulse is weak, and therefore non-linear effects such as two-photon absorption and second harmonic generation are negligible and not observed. Differential reflectivity ΔR/R was obtained from the measured spectra of the reflected probe at various pump and one-photon probe time delays and are presented in Fig. 2, where color code represents normalized changes. We observed two prominent spectral features centered near 1.86 eV and 2.01 eV coinciding with the reported resonance values for the A and B excitons in the MoS_2 monolayers, their energies are marked with the black dotted lines in Fig. 2(a).

Since the monolayer was undoped, trion peaks were not [23] in the reflectivity measurements as well as linear photoluminescence measurements (top inset of Fig. 2(b)). Any population to the higher lying 2-S states also quickly scatter down to the 1-S states due to efficient intra-valley scattering processes [24]. The changes in sample absorption after the pump arrival result in alternating differential reflectivity spectra near the mentioned energy values (Fig. 2(b) lower inset).

The minima of ΔR/R (dashed lines in Fig. 2(a)) were used to extract A and B exciton dynamics shown in Fig. 2(b). The absolute value of ΔR/R decreases monotonically with multi-exponential decay. Such behavior in TMDs has been previously observed in one-photon pump-probe measurements and in time-resolved photoluminescence [7,6,9]. This behavior has been attributed to various types of radiative and non-radiative recombination pathways such as exciton-exciton annihilation process, which depend strongly on the excited carrier density, trap or defect assisted non-radiative recombination, as well as scattering into dark-exciton states [13,24] . The scattering to dark excitonic states is difficult to isolate from all the other aforementioned recombination mechanisms. Thus, the direct measurement of the dark state lifetime is virtually impossible with the standard one-photon excitation techniques.

Optics EXPRESS

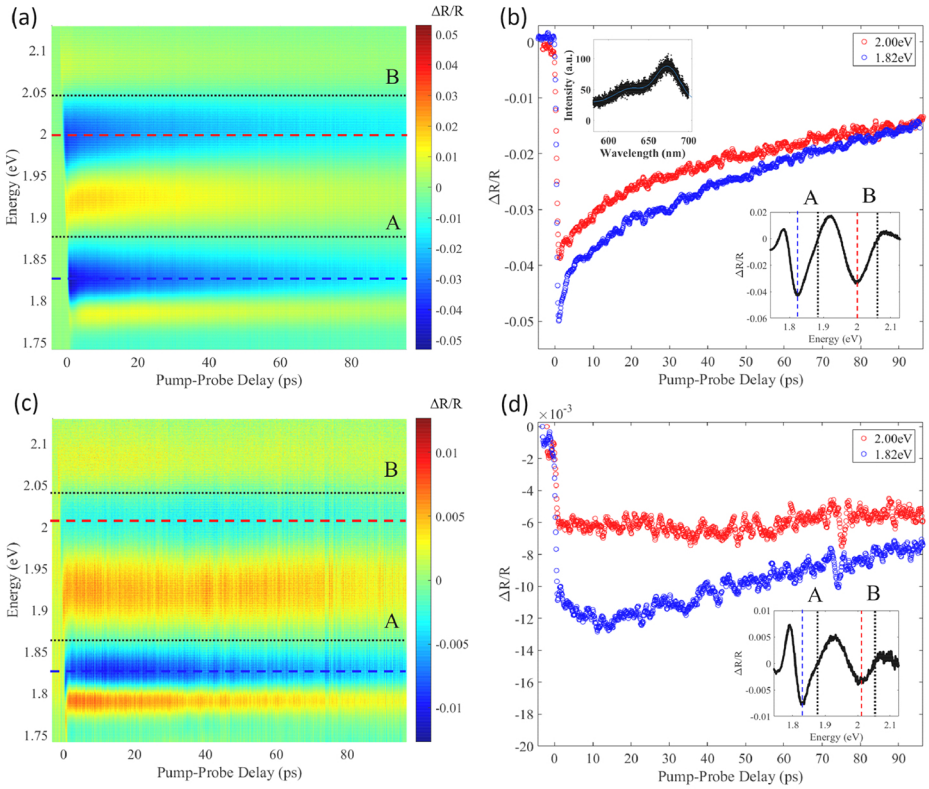

Fig. 2. (a), (c). Differential reflectivity spectra of MoS_2 as a function of energy and pump-probe delay time obtained under one-photon **(a)** and two-photon **(c)** excitation schemes, corresponding to pump photon energies of 2.55 eV and 1.01 eV, respectively. Two prominent features centered at 1.86 eV and 2.01 eV correspond to A and B exciton reflectivity changes caused by the pump. Dotted black lines mark A and B exciton energies. **(b), (d)**. Time evolution of ΔR/R at energies shown in **(a)** and **(c)** by the two dashed lines, which reflects A and B exciton dynamics. Top inset in **(b)** shows linear photoluminescence plot showing no trion peaks. Bottom insets in **(b)** and **(d)** depict ΔR/R as a function of energy close to the zero pump-probe delay time.

Optics EXPRESS

In this work, we use a two-photon excitation technique, which directly populates 2P dark-exciton states [18]. The pump energy in the two-photon pump and one-photon probe experiment was set slightly above half of the 2P A-exciton energy. We excited the sample with a photon energy of 1.01 eV with pump fluence of 6.18 mJ/cm^2, under which two-photon excitation can directly populate 2P state of A-exciton series [18] . The B excitons, lying 20 meV lower than the 2P state are populated [25]. The two-photon absorption selection rule permits selective population of the 2P state and observation of its dynamics to bright states of both A and B excitonic series [18]. Even as the 2S and 2P states are close by in energy, with 2P being slightly lower, the two-photon selection rule selectively populate the 2P state making the population dynamics significantly simpler. The observed dynamics under such excitation is fundamentally different from that obtained under one-photon excitation. Comparing Fig. 2(b) and Fig. 2(d) we stress two important observations, which are related to the central theme of this work: slow and non-monotonic dynamics of the differential reflectivity in the two-photon case. The two-photon differential reflectivity dynamics allow us to directly extract the 2P dark exciton lifetime, determined by 2P $\rightarrow$ 1S scattering times, in these two-dimensional materials. Based on our experimental data analysis, the 2P dark to bright exciton scattering time at room temperature is estimated to be 72.5 ps in monolayer MoS_2. This value is larger than similar dynamics of nP excitons studied in MoS_2 at 77 K using intra-band infra-red excitations by Cha et. al [17]. This longer lifetime observed at room temperature in our measurements can be explained by population dynamics with other dark excitonic species such as spin flip excitons with much longer lifetime [16].

The exciton energy diagram of MoS_2 monolayer and the one- and two-photon excitation schemes implemented in our experiment are shown in Fig. 3. The bright and dark excitonic states appear in orange and in gray respectively. The electron continuum is colored in blue. Under one-photon excitation (2.55 eV), electrons created in the continuum relax, forming bright and dark excitons of all types as shown in Fig. 3(a). The created excitons can further recombine via either radiative or non-radiative processes such as Auger and trap/defect-assisted recombination. The P-type dark excitons can recombine non radiatively, get scattered to low lying 1S bright states [26]. Moreover, spin-flip mechanisms allow scattering from the bright to the spin forbidden dark states and vice versa. In the two-photon excitation case (1.01 eV), in contrast, the pump mostly creates P-type dark excitons directly via two-photon absorption [18] . Thus, the bright-exciton states, measured by the probe pulse, are populated via scattering from the dark states. The bright state population dynamics measured through time dependent differential reflectivity allows us to extract the scattering time from the dark states to the bright ones. The density dynamics of bright exciton population (X_B) and the dark exciton population (P type X_D^P, spin forbidden X_D^S, outside the light cone dark X_D^O) are modeled as follows:

$$\frac{dX_B}{dt} = G_{xB}(t) - R_r X_B - D_t N_t X_B + SF(X_D^S - X_B) + M_{DB} X_D^P - M_{BD} X_B - AX_B^2 + M^o(X_D^o - X_B) \tag{2}$$

$$\frac{dX_D^P}{dt} = G_{xD}(t) + M_{BD} X_B - M_{DB} X_D^P + M^o(X_D^o - X_D^P) - R_{nr} X_D^P \tag{3}$$

$$\frac{dX_D^S}{dt} = SF(X_B - X_D^S) + M^o(X_D^o - X_D^s) - R_{nr} X_D^S \tag{4}$$

$$\frac{dX_D^O}{dt} = -M^o(X_D^o - X_B - X_D^S - X_D^P) - R_{nr} X_D^O \tag{5}$$

$$\frac{dN_t}{dt} = -D_t N_t X_B \tag{6}$$

where, $G_{xB}(t)$ and $G_{xD}(t)$ are generation rates of bright and P-type dark excitons, respectively; R_r is the radiative recombination rate, N_t is the density of available traps and $D_t N_t$ is the Auger recombination rate via traps; SF is the spin forbidden dark $\leftrightarrow$ bright scattering rate, M° is the effective scattering rate to dark excitons which lie outside the light cone, which includes

Optics EXPRESS

scattering to intravalley and intervalley excitons, M_{DB} is the phonon-assisted scattering rate responsible for P-type dark→ bright scattering, and M_{BD} is the scattering rate of 1S to 2P. A is the exciton-exciton annihilation rate and R_{nr} non-radiative recombination rate of dark excitons. Δ is the energy separation between the bright and the P-type dark state. The radiative decay occurs through one-photon emission at a rate proportional to exciton population [6]. On the other hand, many non-radiative pathways exist with varying decay rates [27]. At high carrier densities (in the range of 10^{12} cm^{-2}) exciton-exciton annihilation is efficient [7] and is considered here at a rate of A s^{-1}. The dark excitons are taken to have a non-radiative recombination rate of R_{nr} s^{-1}. Of the many types of Auger recombination pathways, trap assisted Auger was found to be the most dominant in MoS_2 [7]. Here we consider electron-exciton Auger scattering with a decay time constant of D_t. Since it is trap-assisted, the time-dependent density of available traps was also considered. The bright to dark scattering at the rate of SF s^{-1} is used in the model. The exciton dynamics in monolayer transition metal dichalcogenides is complicated and diverse at room temperature. The characteristic lifetimes of individual pathways are different thereby affecting the overall lifetime. While radiative decay rates are fast, processes involving scattering between bright excitons and different types of dark excitons such as spin flipped dark excitons, linear momentum forbidden (out of light cone and inter-valley excitons) and angular momentum forbidden dark excitons are comparatively slower. Spin flipped dark excitons have long lifetime of about 1 ns and hence have much smaller impact on general dynamics. The rate equations are formulated here are used to describe a general scenario and hence, the model includes the spin flip scattering with dark excitons, even as its influence on the actual numbers are small.

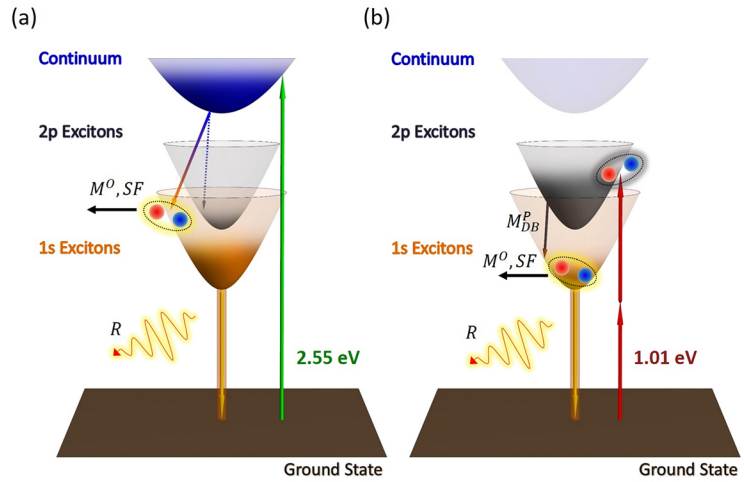

Fig. 3. Monolayer MoS2 exciton band structure and population dynamics under one-photon and two-photon excitations. (a). In the one-photon case (2.55 eV photon energy), continuum states are directly excited and the carriers decay populating both 1S and 2P excitons. (b). In the two-photon case (1.01 eV photon energy), 2P excitons are directly generated and scatter to the 1S states. The reverse process, where the 1s excitons scatters to the dark ones, is less probable due to the energy scales involved. Since the 1S population can be created only from the 2P scattering in this case, the 1S dynamics allows measuring the 2P lifetime directly.

In the one-photon case, $G_{xB}(t) = \alpha_1 I(t)$ and $G_{xD}(t) = 0$, where α_1 is the one-photon absorption efficiency and $I(t)$ is the pump intensity. In the two-photon case $G_{xD} = \alpha_2 I(t)^2$ and $G_{xB}(t) = 0$, where α_2 is the two-photon absorption efficiency. The pulse temporal intensity dependence is well described by Gaussian width FWHM of 35 fs. The time-dependent densities of the

Optics EXPRESS

bright (X_B) and the dark (X_D^P) excitons are obtained by relating the differential reflectivity to the absorption change and including photon to exciton conversion efficiency [7].

The set of equations (2–6) were solved self-consistently and the characteristic times (including the previously unknown 2P dark→ bright scattering time) of various scattering events were obtained from theoretical fits to the experimentally observed differential reflectivity (Table 1).

Table 1. Parameters for rate Eq. 2–6.

Parameters	Life Time (ps)	Error margin (ps)	Rate (ps^{-1})
radiative recombination	132	5	0.0075
2P → bright scattering	72.5	10	0.013

Figure 4(a), and 4(b) present A and B exciton dynamics, respectively, monitored through differential reflectivity temporal changes in the case of 2.55 eV one-photon excitation energy. The pump induced carrier density also leads to renormalization of the exciton energy levels as previously observed [28,29] and the experimentally observed renormalized energy levels and their time dynamics are given as an inset in each case. They match closely with previous reports [29] with excited carrier densities of about 3.5×10^{12} cm^{-2} A excitons and $7.6\times10^{11}cm^{-2}$ B excitons for one-photon excitation and 4.2×10^{11} cm^{-2} and 5×10^{10} cm^{-2} respectively for two photon excitation. The calculated bright and the dark exciton densities are shown in red and gray solid lines, respectively, and match well the measured dynamics. In the one-photon excitation case, the decay is monotonic as the generated bright excitons decay via Auger or radiative pathways as well as via scattering to the underlying bright and dark states. The extracted radiative lifetime, using the previously reported times for exciton-exciton (2×10^{-2} cm^2/s) and trap-assisted Auger scattering (5×10^{-20} cm^6/s), match well with the previously reported values [7,6].

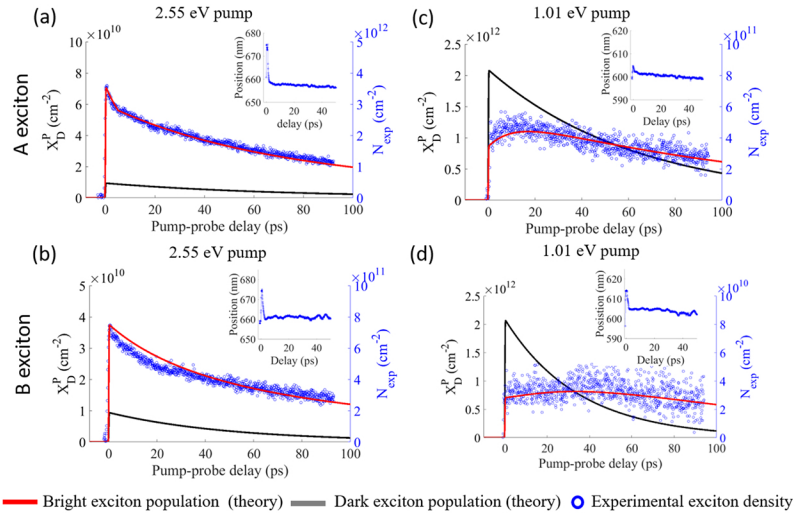

Fig. 4. (a),(b). Temporal A and B exciton density dynamics, respectively, in the case of one-photon excitation with photon energy of 2.55 eV. **(c),(d).** Temporal A and B exciton density dynamics, respectively, in the case of two-photon excitation with photon energy of 1.01 eV. The blue circles are the measured values, the red and the gray lines are the calculated bright and dark exciton densities, respectively. Carrier density dependent renormalization of exciton peak position is given as an inset in each case.

The 2P → 1S bright exciton scattering time was observed to be 72.5 ps. Since the non-radiative recombination is much slower (lifetime to be about 1 ns) the effective lifetime of 2P dark exciton

Optics EXPRESS

state is dominated by the 2P dark → bright scattering rates. Figure 4c and d present A and B exciton dynamics, respectively, in the case of 1.01 eV two-photon excitation energy. Here, it must be noted that in our experiment two-photon excitation can populate only the 2P states of A series, whereas 2P of B exciton is about 170 meV higher than the excitation energy. B-exciton population dynamics observed here is due to indirect population of the 1S B exciton states [26,28]. However, the main difference when comparing with the one-photon case is the non-monotonic bright exciton population dynamics exhibiting a rise in ΔR/R during the first 15 ps for the A exciton and 40 ps for the B exciton and subsequent monotonic decay, significantly longer than the one-photon case decay. Since, the P-type dark excitons have complex population dynamics including several pathways, a detailed rate equation model such as the one described before, in contrast to a much simpler one used in other reports [30], was necessary to extract the exact lifetime. The P-type dark excitons, which are exclusively populated by the two-photon excitation process, are forbidden to decay radiatively via one-photon processes. This makes the 2P dark scattering to the bright states, followed by the bright exciton decay, and recombination via non-radiative processes the most probable pathways for recombination as shown in Fig. 3(b). The bright excitons undergo fast recombination, in comparison to the scattering rate, and thus the dark to bright scattering time, as measured here, strongly determines the dark excitonic lifetime.

4. Conclusions

We demonstrated bright and dark exciton formation and decay using one- and two-photon pump and one-photon probe spectroscopy, and identified the characteristic times of various decay processes. We showed that in MoS_2, the dark excitons are directly generated by the two-photon excitation and undergo 2P dark → bright scattering with a characteristic time of ~72.5 ps. Such direct measurements of radiative and scattering times can aid in better understanding of proposed optoelectronic devices using these novel materials. We believe that the knowledge of the dark exciton formation and scattering times to the bright counterparts could be largely beneficial for devices based on quantum memory and other valleytronic/valley-optoelectronic applications. With the help of the constructed model, one can predict the lifetimes of various processes such as defect/trap mediated Auger recombination and radiative recombination to engineer highly efficient light emitters, photodetectors, and solar cells.

Funding

Israel Science Foundation (1363/15, 1995/17, 2220/15, 934/18).

References

1. S. Manzeli, D. Ovchinnikov, D. Pasquier, O. V. Yazyev, and A. Kis, "2D transition metal dichalcogenides," Nat. Rev. Mater. **2**(8), 17033 (2017).
2. Y. K. Srivastava, A. Chaturvedi, M. Manjappa, A. Kumar, G. Dayal, C. Kloc, and R. Singh, "MoS2 for Ultrafast All-Optical Switching and Modulation of THz Fano Metaphotonic Devices," Adv. Opt. Mater. **5**(23), 1700762 (2017).
3. K. F. Mak and J. Shan, "Photonics and optoelectronics of 2D semiconductor transition metal dichalcogenides," Nat. Photonics **10**(4), 216–226 (2016).
4. T. Cao, G. Wang, W. Han, H. Ye, C. Zhu, J. Shi, Q. Niu, P. Tan, E. Wang, B. Liu, and J. Feng, "Valley-selective circular dichroism of monolayer molybdenum disulphide," Nat. Commun. **3**(1), 887 (2012).
5. K. F. Mak, K. L. McGill, J. Park, and P. L. McEuen, "The valley Hall effect in MoS2 transistors," Science **344**(6191), 1489–1492 (2014).
6. H. Wang, C. Zhang, W. Chan, C. Manolatou, S. Tiwari, and F. Rana, "Radiative lifetimes of excitons and trions in monolayers of the metal dichalcogenide MoS 2," Phys. Rev. B **93**(4), 045407 (2016).
7. H. Wang, C. Zhang, and F. Rana, "Ultrafast dynamics of defect-assisted electron–hole recombination in monolayer MoS2," Nano Lett. **15**(1), 339–345 (2015).
8. G. Moody, C. K. Dass, K. Hao, C.-H. Chen, L.-J. Li, A. Singh, K. Tran, G. Clark, X. Xu, G. Berghäuser, E. Malic, A. Knorr, and X. Li, "Intrinsic homogeneous linewidth and broadening mechanisms of excitons in monolayer transition metal dichalcogenides," Nat. Commun. **6**(1), 8315 (2015).

Optics EXPRESS

9. H. Shi, R. Yan, S. Bertolazzi, J. Brivio, B. Gao, A. Kis, D. Jena, H. G. Xing, and L. Huang, "Exciton dynamics in suspended monolayer and few-layer MoS2 2D crystals," ACS Nano **7**(2), 1072–1080 (2013).
10. M. Palummo, M. Bernardi, and J. C. Grossman, "Exciton radiative lifetimes in two-dimensional transition metal dichalcogenides," Nano Lett. **15**(5), 2794–2800 (2015).
11. T. Korn, S. Heydrich, M. Hirmer, J. Schmutzler, and C. Schüller, "Low-temperature photocarrier dynamics in monolayer MoS2," Appl. Phys. Lett. **99**(10), 102109 (2011).
12. X.-X. Zhang, Y. You, S. Y. F. Zhao, and T. F. Heinz, "Experimental evidence for dark excitons in monolayer WSe 2," Phys. Rev. Lett. **115**(25), 257403 (2015).
13. G. Wang, A. Chernikov, M. M. Glazov, T. F. Heinz, X. Marie, T. Amand, and B. Urbaszek, "Colloquium: Excitons in atomically thin transition metal dichalcogenides," Rev. Mod. Phys. **90**(2), 021001 (2018).
14. J. P. Echeverry, B. Urbaszek, T. Amand, X. Marie, and I. C. Gerber, "Splitting between bright and dark excitons in transition metal dichalcogenide monolayers," Phys. Rev. B **93**(12), 121107 (2016).
15. C. Robert, T. Amand, F. Cadiz, D. Lagarde, E. Courtade, M. Manca, T. Taniguchi, K. Watanabe, B. Urbaszek, and X. Marie, "Fine structure and lifetime of dark excitons in transition metal dichalcogenide monolayers," Phys. Rev. B **96**(15), 155423 (2017).
16. M. R. Molas, C. Faugeras, A. O. Slobodeniuk, K. Nogajewski, M. Bartos, D. M. Basko, and M. Potemski, "Brightening of dark excitons in monolayers of semiconducting transition metal dichalcogenides," 2D Mater. **4**(2), 021003 (2017).
17. S. Cha, J. H. Sung, S. Sim, J. Park, H. Heo, M.-H. Jo, and H. Choi, "1s-intraexcitonic dynamics in monolayer MoS 2 probed by ultrafast mid-infrared spectroscopy," Nat. Commun. **7**(1), 10768 (2016).
18. Z. Ye, T. Cao, K. O'Brien, H. Zhu, X. Yin, Y. Wang, S. G. Louie, and X. Zhang, "Probing excitonic dark states in single-layer tungsten disulphide," Nature **513**(7517), 214–218 (2014).
19. E. Malic, M. Selig, M. Feierabend, S. Brem, D. Christiansen, F. Wendler, A. Knorr, and G. Berghäuser, "Dark excitons in transition metal dichalcogenides," Phys. Rev. B **2**(1), 014002 (2018).
20. C. Jiang, W. Xu, A. Rasmita, Z. Huang, K. Li, Q. Xiong, and W.-b. Gao, "Microsecond dark-exciton valley polarization memory in two-dimensional heterostructures," Nat. Commun. **9**(1), 753 (2018).
21. T. Heindel, A. Thoma, I. Schwartz, E. R. Schmidgall, L. Gantz, D. Cogan, M. Strauß, P. Schnauber, M. Gschrey, J.-H. Schulze, A. Strittmatter, S. Rodt, D. Gershoni, and S. Reitzenstein, "Accessing the dark exciton spin in deterministic quantum-dot microlenses," APL Photonics **2**(12), 121303 (2017).
22. B. E. A. Saleh, M. C. Teich, and B. E. Saleh, Fundamentals of photonics, vol. 22, Wiley, New York, 1991.
23. K. F. Mak, K. He, C. Lee, G. H. Lee, J. Hone, T. F. Heinz, and J. Shan, "Tightly bound trions in monolayer MoS2," Nat. Mater. **12**(3), 207–211 (2013).
24. A. Tanaka, N. J. Watkins, and Y. Gao, "Hot-electron relaxation in the layered semiconductor," Phys. Rev. B **67**(11), 113315 (2003).
25. B. R. Carvalho, Y. Wang, S. Mignuzzi, D. Roy, M. Terrones, C. Fantini, V. H. Crespi, L. M. Malard, and M. A. Pimenta, "Intervalley scattering by acoustic phonons in two-dimensional MoS2 revealed by double-resonance Raman spectroscopy," Nat. Commun. **8**(1), 14670 (2017).
26. G. Kioseoglou, A. T. Hanbicki, M. Currie, A. L. Friedman, D. Gunlycke, and B. T. Jonker, "Valley polarization and intervalley scattering in monolayer MoS2," Appl. Phys. Lett. **101**(22), 221907 (2012).
27. C. Pöllmann, P. Steinleitner, U. Leierseder, P. Nagler, G. Plechinger, M. Porer, R. Bratschitsch, C. Schüller, T. Korn, and R. Huber, "Resonant internal quantum transitions and femtosecond radiative decay of excitons in monolayer WSe 2," Nat. Mater. **14**(9), 889–893 (2015).
28. R. Schmidt, G. Berghäuser, R. Schneider, M. Selig, P. Tonndorf, E. Malić, A. Knorr, S. Michaelis de Vasconcellos, and R. Bratschitsch, "Ultrafast Coulomb-Induced Intervalley Coupling in Atomically Thin WS2," Nano Lett. **16**(5), 2945–2950 (2016).
29. L. Meckbach, T. Stroucken, and S. W. Koch, "Giant excitation induced bandgap renormalization in TMDC monolayers," Appl. Phys. Lett. **112**(6), 061104 (2018).
30. A. Singh, G. Moody, K. Tran, M. E. Scott, V. Overbeck, G. Berghäuser, J. Schaibley, E. J. Seifert, D. Pleskot, N. M. Gabor, J. Yan, D. G. Mandrus, M. Richter, E. Malic, X. Xu, and X. Li, "Trion formation dynamics in monolayer transition metal dichalcogenides," Phys. Rev. B **93**(4), 041401 (2016).